



Published in final edited form as:

*Science*. 2007 October 12; 318(5848): 274–279. doi:10.1126/science.1146447.

## PKA Type II $\alpha$ Holoenzyme Reveals a Combinatorial Strategy for Isoform Diversity

Jian Wu<sup>1</sup>, Simon H. J. Brown<sup>1</sup>, Sventja von Daake<sup>1</sup>, and Susan S. Taylor<sup>1,2,\*</sup>

<sup>1</sup>Department of Chemistry and Biochemistry, University of California, San Diego, La Jolla, CA 92093, USA

<sup>2</sup>Howard Hughes Medical Institute, University of California, San Diego, La Jolla, CA 92093, USA

### Abstract

The catalytic (C) subunit of cyclic adenosine monophosphate (cAMP)–dependent protein kinase (PKA) is inhibited by two classes of regulatory subunits, RI and RII. The RII subunits are substrates as well as inhibitors and do not require adenosine triphosphate (ATP) to form holoenzyme, which distinguishes them from RI subunits. To understand the molecular basis for isoform diversity, we solved the crystal structure of an RII $\alpha$  holoenzyme and compared it to the RI $\alpha$  holoenzyme. Unphosphorylated RII $\alpha$  (90–400), a deletion mutant, undergoes major conformational changes as both of the cAMP-binding domains wrap around the C subunit's large lobe. The hallmark of this conformational reorganization is the helix switch in domain A. The C subunit is in an open conformation, and its carboxyl-terminal tail is disordered. This structure demonstrates the conserved and isoform-specific features of RI and RII and the importance of ATP, and also provides a new paradigm for designing isoform-specific activators or antagonists for PKA.

---

Cyclic adenosine monophosphate (cAMP) is a universal signal for environmental stress. In mammalian cells, major receptors for cAMP are the regulatory (R) subunits of cAMP-dependent protein kinase (PKA) (1, 2). All R subunits share the same domain organization that includes a dimerization/docking (D/D) domain at the N terminus and two tandem C-terminal cAMP-binding (CNB) domains (domains A and B). The linker joining the D/D and CNB domains is highly disordered in dissociated dimers (3) and contains an inhibitor site that resembles a peptide substrate and docks to the active site of the catalytic (C) subunit in the holoenzyme, thereby blocking its activity.

The two major classes of R subunit (I and II) each have  $\alpha$  and  $\beta$  isoforms. The isoforms are functionally nonredundant, and isoform diversity is a primary mechanism for achieving specificity in PKA signaling (4). The inhibitor site is a distinguishing feature of the

---

\*To whom correspondence should be addressed. staylor@ucsd.edu.

#### Supporting Online Material

[www.sciencemag.org/cgi/content/full/318/5848/274/DC1](http://www.sciencemag.org/cgi/content/full/318/5848/274/DC1)

Materials and Methods

Figs. S1 to S6

Tables S1 and S2

References

isoforms. RII subunits have a phosphorylation site in their inhibitor motif and thus are both substrates and inhibitors, whereas RI subunits with Ala or Gly at the P-site are pseudo-substrates. RI subunits require ATP and two  $Mg^{2+}$  ions to form a stable holoenzyme complex (binding affinity  $K_d = 0.1$  nM) (5), whereas RII subunits do not ( $K_d = 0.1$  nM).

Although the structures of the open and closed conformations of the C subunit (6, 7) and the cAMP-bound structures of RI $\alpha$  and RII $\beta$  (8, 9) have been solved, they do not explain how C is inhibited by R, how the holoenzyme is activated by cAMP, and how the isoforms differ. To understand the molecular basis for differential regulation of type I and type II holoenzymes, we purified a deletion mutant of RII $\alpha$ , RII $\alpha$ (90–400), and cocrystallized it with the C $\alpha$  subunit in the absence of ATP, then compared it to the RI $\alpha$  holoenzyme (10, 11). In contrast to the C subunit's fully closed conformation in the type I holoenzyme, in the RII $\alpha$  complex the C subunit is in an open conformation, the ATP binding pocket is empty, the  $\alpha$ B/ $\alpha$ C helix is distorted, and the C-terminal tail is disordered. Like RI $\alpha$ , RII $\alpha$  undergoes major conformational changes as it wraps around the large lobe of the C subunit. The hallmarks of this conformational switch are changes associated with the helical subdomains of both cAMP-binding domains. Most striking is the helix switch in domain A, which snaps apart the two CNB domains. In the holoenzyme, domain B of RII $\alpha$  docks onto the  $\alpha$ H- $\alpha$ I loop of the C subunit.

This structure demonstrates the combinatorial diversity of the C subunit as it uses diverse sets of docking motifs to interact in unique ways with different inhibitors, and we presume that this diversity is also related to recognition of different protein substrates. The structure also demonstrates how ATP differentially regulates these two holoenzymes. ATP is essential for forming the type I holoenzyme, much as guanosine triphosphate (GTP) is essential for generating the active conformation of heterotrimeric GTP-binding proteins (G proteins), whereas in type II holoenzymes, ATP, through autophosphorylation, actually promotes dissociation.

A monomeric deletion mutant of RII $\alpha$  was cocrystallized with the wild-type C $\alpha$  subunit in the absence of  $Mg_2ATP$  (for statistics, see table S1). The structure reveals a large interface that engages the entire RII $\alpha$  subunit but only the large lobe of the C subunit (Fig. 1). The C subunit, with the exception of a distorted  $\alpha$ B- $\alpha$ C loop, assumes an open conformation. The active-site cleft is open and the C-terminal tail (residues 319 to 331) is disordered (Figs. 2 and 3). The inhibitor site and linker region, which are disordered in the free RII subunit, become ordered in the holoenzyme. Docking of domain A onto the large lobe of the C subunit creates an extended interface, whereas domain B contributes a small but essential docking motif that binds to the  $\alpha$ H- $\alpha$ I loop on the C subunit (Fig. 1, B and C).

The large lobe of the C subunit functions as a stable scaffold for RII $\alpha$ , with the binding interface extending from the common inhibitor binding site at the active-site cleft, over the activation loop and the P+1 loop, to the  $\alpha$ H- $\alpha$ I loop (Fig. 1 and fig. S1). ATP is not required for this high-affinity binding ( $\sim 1.0$  nM). The C subunit is in an open conformation similar to that of the apoenzyme (6) (Fig. 2 and fig. S2). The small lobe is more dynamic than the large lobe, as indicated by the disorder of many side chains and the discontinuity of the C-terminal tail. Comparison of average temperature factors (*B* factors) for the RII $\alpha$  and RI $\alpha$

holoenzymes reveals a striking isoform difference in dynamics (Fig. 3C). In both holoenzymes there is 70% water content, and crystal packing does not influence the small lobe.

In contrast to the C subunit, RII $\alpha$  undergoes major conformational changes in almost its entire molecular architecture relative to the unbound structure. Each domain contains  $\alpha$  and  $\beta$  sub-domains. The  $\beta$  sandwich harbors the signature motif of the CNB, the phosphate-binding cassette (PBC), where the phosphate moiety of cAMP docks. The release of cAMP uncouples the  $\alpha$  and  $\beta$  subdomains (12), thus allowing for global conformational changes in the helices that are induced and stabilized by binding of the C subunit. RII $\alpha$  undergoes three major changes: (i) ordering of the inhibitor peptide and the following linker segment; (ii) reorganization of the helical subdomains of domain A, which leads to the separation of domains A and B; and (iii) reorganization of the helical subdomain of domain B to accommodate docking to the  $\alpha$ H- $\alpha$ I loop in the C subunit. With this structure we can appreciate the conservation of the dynamic uncoupling of the A and B domains as they release cAMP and bind to the C subunit.

For simplicity, we divide the large R-C interface into four distinct sites on the C subunit (Fig. 1). Site 1, where the inhibitor peptide docks to the active-site cleft, most clearly distinguishes the R-subunit isoforms. Site 2 is dominated by the  $\alpha$ G helix and the P+1 loop, site 3 includes the activation loop and the APE- $\alpha$ F loop, and site 4 is the  $\alpha$ H- $\alpha$ I loop. The RII-specific features of sites 1 and 4 are described in detail below; sites 2 and 3 are discussed in (13).

Because RII subunits are substrates as well as inhibitors, they engage the active-site cleft differently from RI $\alpha$  subunits. RII $\alpha$ (90–400) begins with Arg<sup>92R</sup>-Arg-Val-Ser-Val<sup>96R</sup>, where Ser<sup>95R</sup> is the unphosphorylated P-site. (For clarity, we adopt a nomenclature where residues from the R and C subunits are respectively designated by superscripts R and C.) The positions of the backbone and side chains in this segment are nearly identical to those of the protein kinase inhibitor peptide PKI(5–24) and RI $\alpha$ , even though both PKI and RI $\alpha$ , with Ala at the P-site, are pseudo-substrates (Fig. 3). The C subunit in the RII $\alpha$  holoenzyme structure assumes an open conformation, in contrast to the fully closed conformation found in the PKI(5–24)–C complex (7) and the RI $\alpha$  holoenzyme (10, 11). Because the RII $\alpha$  and C subunits were cocrystallized in the absence of MgATP, there is no phosphate on Ser<sup>95R</sup>. In the presence of ATP the inhibitor site would undergo autophosphorylation, which reduces the affinity of RII $\alpha$  for the C subunit (14).

A major isoform difference is that each residue from the five-residue peptide is docked firmly onto the large lobe; neither the small lobe nor the C-terminal tail is involved (Fig. 2C and fig. S2). In contrast, recruitment of the small lobe and the C-terminal tail are essential for RI $\alpha$  and PKI, where the  $\gamma$ -phosphate of ATP is trapped between the two lobes, as it is in the transition state during catalysis (15). Instead, in the RII $\alpha$  holoenzyme, the P-site Ser forms hydrogen bonds with catalytic loop residues that are anchored to the P+1 loop (Fig. 2C).

The P+1 Val, disordered in the free RII subunit, docks onto the P+1 loop and nucleates the hydrophobic interface between RII $\alpha$  and C by interacting with Tyr<sup>247C</sup> in the  $\alpha$ G helix of C and Tyr<sup>209R</sup> in the PBC of RII $\alpha$  (fig. S1). Although Tyr<sup>247C</sup> does not change much relative to its position in the free C subunit, Tyr<sup>209R</sup> is recruited because of the rearrangement of domain A. This hydrophobic docking surface, which is similar to RI $\alpha$  (10, 11), is discussed in (13).

In addition to the P-site residue, the linker regions account for considerable variation in overall organization of full-length RI and RII subunits and their corresponding holoenzymes (16–18). In previous cAMP-bound structures of RI $\alpha$  and RII $\beta$ , the linker region was always disordered (8, 9). Figure 3 and fig. S3 highlight some of the RII-specific interactions in this region. Glu<sup>99R</sup>, for example, causes a distortion of the  $\alpha$ B- $\alpha$ C loop relative to all previous C-subunit structures (Fig. 2) and is essential for forming type II, but not type I, holoenzymes (19). The importance of other RII-specific sites in the linker is discussed in (13).

The  $\alpha$ H- $\alpha$ I loop (Fig. 1, B and C) is an important docking site for domain B. This region contains a five-residue insert (residues 282<sup>C</sup> to 287<sup>C</sup>) that is unique to the AGC kinases (20). It also contains Arg<sup>280C</sup>, the last highly conserved residue in the kinase core, which forms ion pairs with Glu<sup>208C</sup> in the APE motif at the end of the P+1 loop. Recent genetic studies suggest that there is feedback between this region and the peptide recognition site (21). This site is thus likely to be a “hot spot” for allosteric regulation at several levels.

When holoenzyme forms, major changes take place in the CNB domains of RII $\alpha$ . The global change in architecture that splays apart domains A and B is due to the long contiguous helix that is formed by the merging of the  $\alpha$ B and  $\alpha$ C helices in domain A (Fig. 4 and fig. S4). Changes in domain B are also substantial but different (figs. S4 and S5). Both hydrophobic capping residues for cAMP lie in domain B and are displaced by this movement. In contrast to the helical subdomains, both  $\beta$  subdomains are stable with the exception of the PBC.

Domain A provides the major isoform-independent docking surface for the C subunit and also mediates the global reorganization of the two CNBs. The most striking change is the “ $\alpha$ B/ $\alpha$ C switch” where the kinked  $\alpha$ B and  $\alpha$ C helices of the cAMP-bound state snap into a fully extended single helix. This  $\alpha$ B/ $\alpha$ C switch, a conserved feature of both isoforms (Fig. 4 and fig. S4), not only separates the two CNB domains but also removes the capping residue for site A. The  $\alpha$ B/ $\alpha$ C motif provides a major interacting surface for docking to the C subunit (Fig. 1D) as well as to the linker region (fig. S3), with many residues previously exposed to solvent now serving to nucleate the RII $\alpha$ -C interface (13).

In addition to being “flipped away” from domain A, domain B also undergoes major conformational changes within its helical subdomain. In domain B of RII $\alpha$  the hydrophobic capping residue for cAMP is Tyr<sup>381R</sup>, which is located within its own  $\alpha$ C helix, similar to catabolite activator protein (CAP) (22); in the holoenzyme, Tyr<sup>381R</sup> is no longer close to the PBC because of the conformational changes (Fig. 4). However, the  $\alpha$ C helix does not fuse with the  $\alpha$ B helix but forms a helix-turn-helix ( $\alpha$ C'- $\alpha$ C'') motif (Fig. 4B and fig. S4). In the holoenzyme, Tyr<sup>381R</sup> is exposed to solvent.

Although the cAMP-bound structures of RI $\alpha$  and RII $\beta$  enabled the identification of residues essential for cAMP binding (8, 9), the functions of other conserved residues were not explained. Their conserved functions are revealed only by the two holoenzyme structures. Arg<sup>376R</sup> is an example. The electrostatic contact between Arg<sup>376R</sup> in the  $\alpha$ C helix and Glu<sup>265R</sup> in the  $\alpha$ A helix of domain B is a conserved feature of both holoenzymes, whereas in the cAMP-bound state both residues are exposed to solvent. This electrostatic interaction stabilizes the capping residues in both holoenzyme conformations, even though the location of the A-site capping residue is isoform-specific (Fig. 4B). Arg<sup>365R</sup> in the  $\alpha$ B helix is a conserved part of the R-C interface for both holoenzymes, where it forms essential multivalent interactions with Lys<sup>285C</sup> in the AGC-specific insert that lies in the  $\alpha$ H- $\alpha$ I loop (Fig. 1C). In RII subunits, however, Arg<sup>365R</sup> is also the capping residue for cAMP bound to site A. Other residues such as Arg<sup>213R</sup> and Glu<sup>204R</sup> in the PBC play a conserved role in binding cAMP but are exposed to solvent in the holoenzymes. The roles of many key residues in each conformational state are summarized in table S2.

A tyrosine at the tip of the PBC is another highly conserved feature of A domains. In both holoenzyme structures this tyrosine is essential for docking to C (figs. S1 and S4). The environment of this tyrosine, however, is isoform-specific. In RII $\alpha$  Tyr<sup>209R</sup> is part of an extended hydrogen-bonding network, where it anchors the PBC of domain A to two essential elements in the helical subdomain of domain B. In RI $\alpha$ , Tyr<sup>205R</sup> is exposed to solvent (fig. S4).

Comparison of the holoenzyme structures shows the wide dynamic range of the CNB domains (23). The A domains in both RI and RII are similar in their cAMP and holoenzyme conformations. The B domains are also similar. However, the holoenzyme conformations of the A and B domains are different from each other (fig. S5). Thus, there is not a conserved mechanism for snapping open the  $\alpha$ B- $\alpha$ C helix into a single fused helix.

To appreciate the versatility of the C subunit, one needs to consider it as a scaffold. Figure 4C and fig. S6 summarize the different parts of the C subunit that can be recruited to recognize its inhibitors (RI, RII, and PKI). Each inhibitor must accomplish two things: It must bind with high affinity and also must inhibit catalytic activity. A substrate-like inhibitor sequence is required for inhibition but is not sufficient for high-affinity binding. For both R subunits to achieve high-affinity binding, docking of domain A to the large lobe of the C subunit (sites 2/3) is essential; however, this is not sufficient. In addition to domain A, RI subunits require the N-lobe and C-tail coupled through Mg<sub>2</sub>ATP to the inhibitor site (24), whereas RII subunits require site 4 coupled to domain B. Like RI $\alpha$ , PKI uses the N-lobe and C-tail plus Mg<sub>2</sub>ATP, but achieves high affinity by using another site entirely, the  $\alpha$ F- $\alpha$ G loop (site 5) (7).

RI subunits and PKI both induce a fully closed conformation and require Mg<sub>2</sub>ATP (5), where the  $\gamma$ -phosphate of ATP brings together both lobes (Fig. 4C). Because the inhibitor peptide is a pseudo-substrate and lacks a P-site acceptor, ATP traps the complex in an inactive state, much as GTP traps G proteins in an active state. Formation of RII holoenzyme does not require the N-lobe, the C-tail, or Mg<sub>2</sub>ATP. Because the P-site is a Ser, RII subunits cannot trap the R-C complex in a stable transition state; instead, the P-site Ser

is anchored to the large lobe (Fig. 4C). For RII holoenzymes, ATP facilitates dissociation through autophosphorylation of the P-site rather than stabilizing the inhibited state (14). A corollary for these two models is that RII holoenzymes depend exclusively on cAMP for activation, whereas RI holoenzymes can be regulated by Mg and ATP as well as by cAMP. These two holoenzymes provide a basis for designing novel isoform-specific activators and inhibitors of PKA.

## Supplementary Material

Refer to Web version on PubMed Central for supplementary material.

## Acknowledgments

We thank the Advanced Light Source for assistance in data collection, E. Radzio-Andzelm for assistance in preparation of the figures, and M. Deal for purification of the C subunit. Supported by NIH grant GM34921 (S.S.T.) and NIH training grant T32-CA009524 (S.H.J.B.). The coordinate and structure factor are deposited with the Protein Data Bank (PDB accession code 2QVS).

## References and Notes

- Gill GN, Garren LD. Proc. Natl. Acad. Sci. U.S.A. 1971; 68:786. [PubMed: 4323789]
- Taylor SS, Buechler JA, Yonemoto W. Annu. Rev. Biochem. 1990; 59:971. [PubMed: 2165385]
- Li F, et al. Biochemistry. 2000; 39:15626. [PubMed: 11112551]
- Amieux PS, McKnight GS. Ann. N.Y. Acad. Sci. 2002; 968:75. [PubMed: 12119269]
- Herberg FW, Taylor SS. Biochemistry. 1993; 32:14015. [PubMed: 8268180]
- Akamine P, et al. J. Mol. Biol. 2003; 327:159. [PubMed: 12614615]
- Zheng J, et al. Acta Crystallogr. D. 1993; 49:362. [PubMed: 15299527]
- Su Y, et al. Science. 1995; 269:807. [PubMed: 7638597]
- Diller TC, Madhusudan, Xuong NH, Taylor SS. Structure. 2001; 9:73. [PubMed: 11342137]
- Kim C, Xuong NH, Taylor SS. Science. 2005; 307:690. [PubMed: 15692043]
- Kim C, Cheng CY, Saldanha SA, Taylor SS. Cell. 2007; 130:1032. [PubMed: 17889648]
- Das R, et al. Proc. Natl. Acad. Sci. U.S.A. 2007; 104:93. [PubMed: 17182741]
- See supporting material on *Science* Online.
- Erllichman J, Rosenfeld R, Rosen OM. J. Biol. Chem. 1974; 249:5000. [PubMed: 4367815]
- Madhusudan, et al. Nat. Struct. Biol. 2002; 9:273. [PubMed: 11896404]
- Vigil D, et al. J. Mol. Biol. 2004; 337:1183. [PubMed: 15046986]
- Vigil D, Blumenthal DK, Taylor SS, Trewhella J. J. Biol. Chem. 2005; 280:35521. [PubMed: 16109722]
- Heller WT, et al. J. Biol. Chem. 2004; 279:19084. [PubMed: 14985329]
- Gibson RM, Ji-Buechler Y, Taylor SS. J. Biol. Chem. 1997; 272:16343. [PubMed: 9195940]
- Kannan N, Haste N, Taylor SS, Neuwald AF. Proc. Natl. Acad. Sci. U.S.A. 2007; 104:1272. [PubMed: 17227859]
- Deminoff SJ, Howard SC, Hester A, Warner S, Herman PK. Genetics. 2006; 173:1909. [PubMed: 16751660]
- Berman HM, et al. Proc. Natl. Acad. Sci. U.S.A. 2005; 102:45. [PubMed: 15618393]
- Rehmann H, Wittinghofer A, Bos JL. Nat. Rev. Mol. Cell Biol. 2007; 8:63. [PubMed: 17183361]
- Huang LJ, Taylor SS. J. Biol. Chem. 1998; 273:26739. [PubMed: 9756917]
- Abbreviations for amino acid residues: A, Ala; C, Cys; D, Asp; E, Glu; F, Phe; G, Gly; H, His; I, Ile; K, Lys; L, Leu; M, Met; N, Asn; P, Pro; Q, Gln; R, Arg; S, Ser; T, Thr; V, Val; W, Trp; Y, Tyr.

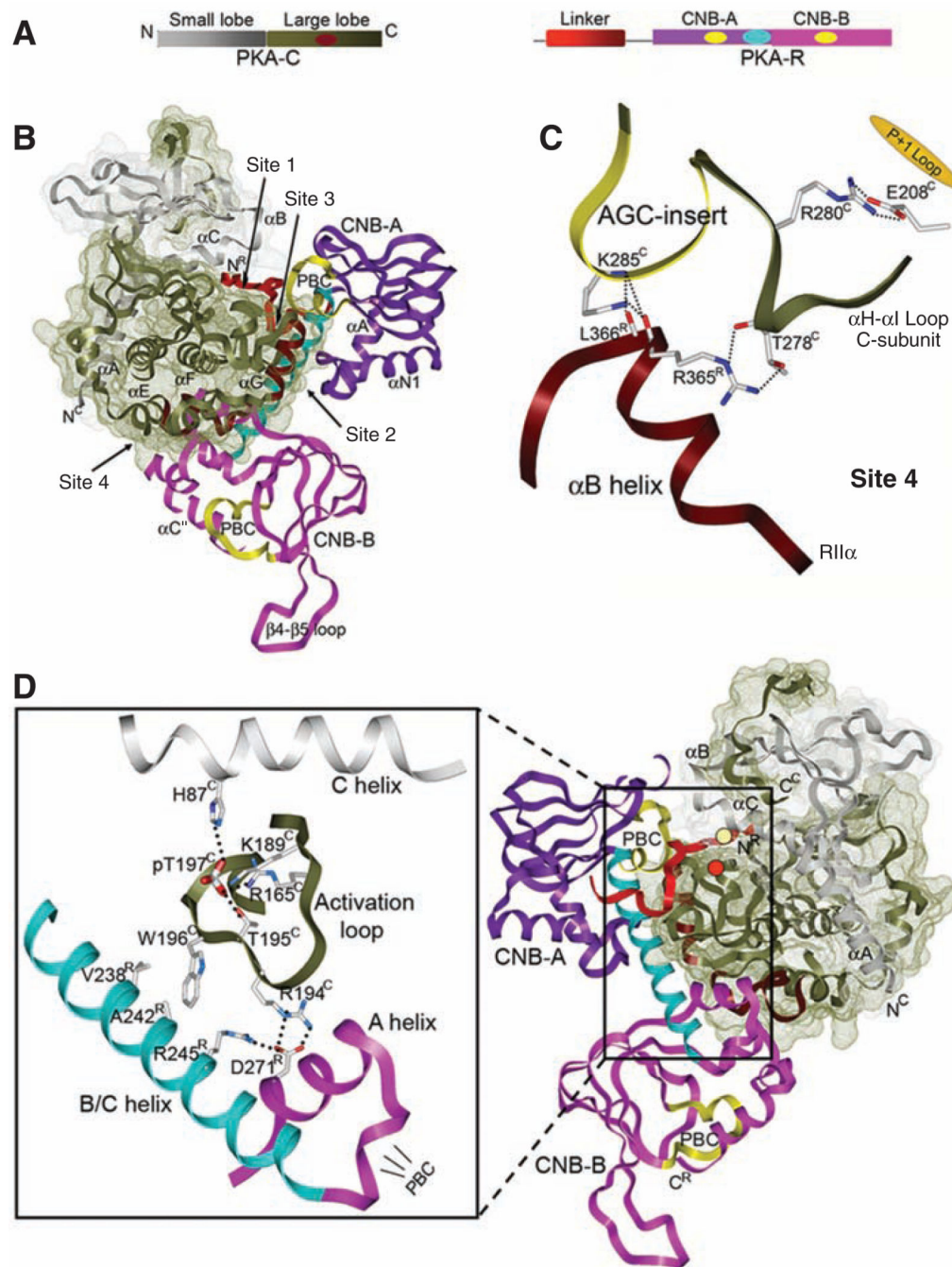


**Fig. 1.** Overall architecture of the RII $\alpha$ (90–400)–C holoenzyme. (A) General domain organization and color coding for the R and C subunits. The small and large lobes of C are shown in gray and tan, respectively, with the position of the  $\alpha$ G and  $\alpha$ H- $\alpha$ I loops highlighted in dark red. The A and B domains of R are in purple and magenta, respectively, with the linker region in red,  $\alpha$ B- $\alpha$ C in cyan, and the two PBCs in yellow. (B) The RII $\alpha$  holoenzyme structure with the C subunit shown in its classic view with a shadowed space-filling surface. Site 1 (inhibitor site), site 2 ( $\alpha$ B helix and P+1 loop), site 3 (activation loop and APE- $\alpha$ F loop),

and site 4 ( $\alpha$ H- $\alpha$ I loop) are indicated. Helices are labeled periodically to help track the Ca trace. **(C)** Essential features of site 4. The  $\alpha$ B helix of RII $\alpha$  (dark red) is shown docked to the  $\alpha$ H- $\alpha$ I loop in C (tan). The AGC-specific insert is highlighted in yellow. The Arg<sup>280C</sup>-Glu<sup>208C</sup> ion pair connecting the  $\alpha$ H- $\alpha$ I loop to the P+1 loop is also shown. **(D)** The 180° rotation of the complex, with the red and yellow circles indicating pThr<sup>197C</sup> and the P-site Ser of RII $\alpha$ , respectively. Expanded at the left are the essential elements of the R-C interface: the  $\alpha$ C helix and activation loop of C, as well as the  $\alpha$ B/ $\alpha$ C helix and the  $\alpha$ A helix of domain B in RII $\alpha$ .



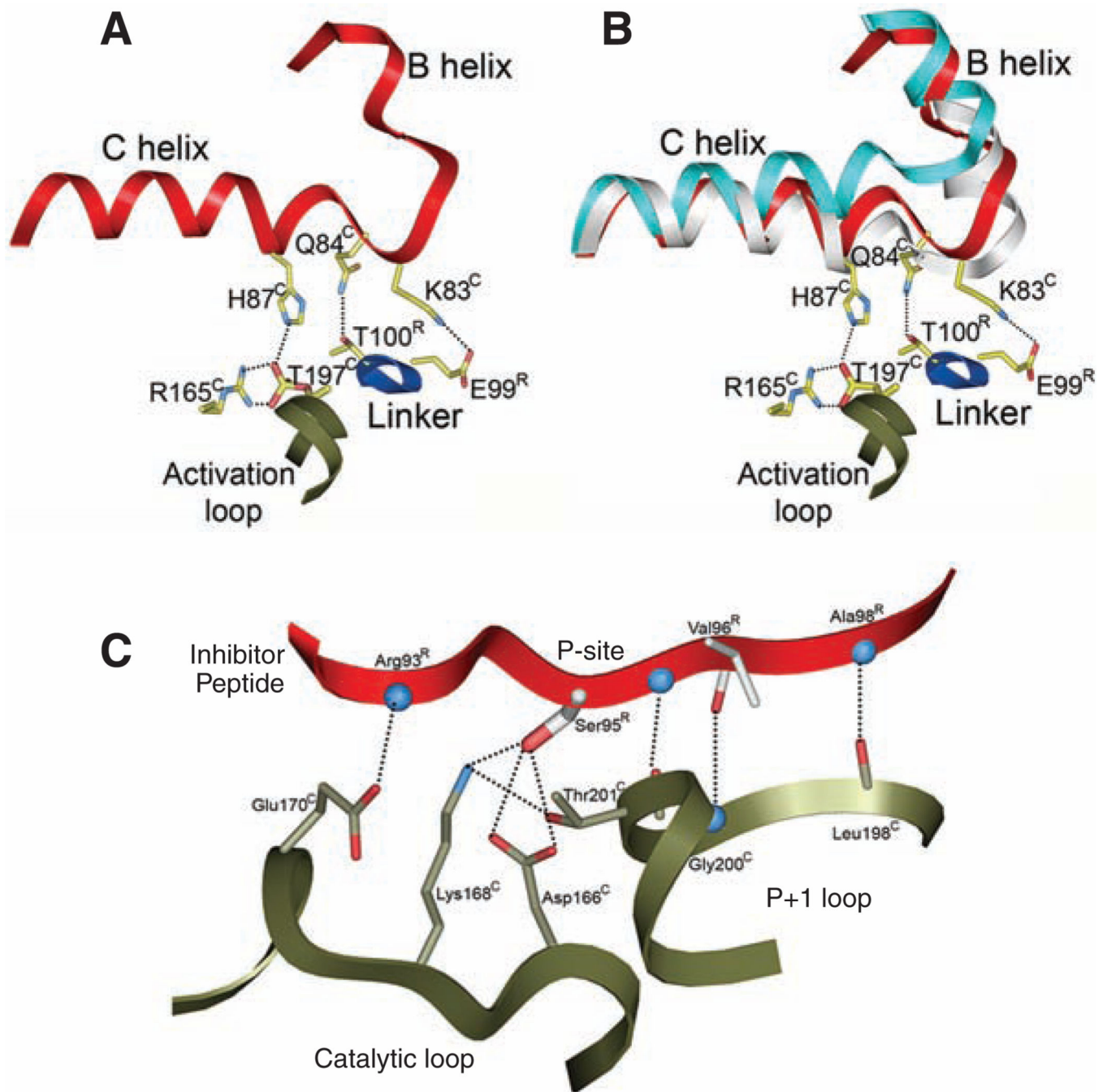


**Fig. 2.** The C subunit is in an open conformation. (A) The H-bond interactions between the  $\alpha$ B and  $\alpha$ C helices with activation loop and RII $\alpha$  linker are indicated in dashed lines. (B) Comparison of the  $\alpha$ B- $\alpha$ C segment to the same region in the wild-type apoenzyme (in cyan) and a closed state of the C subunit (in white). (C) P-site Ser is centered on the preformed active site. In the absence of MgATP, Ser<sup>95R</sup>, the P-site residue, forms hydrogen bonds with Asp<sup>166</sup>C and Lys<sup>168</sup>C from the catalytic loop. The peptide forms a short antiparallel  $\beta$  strand with a segment of the P+1 loop.

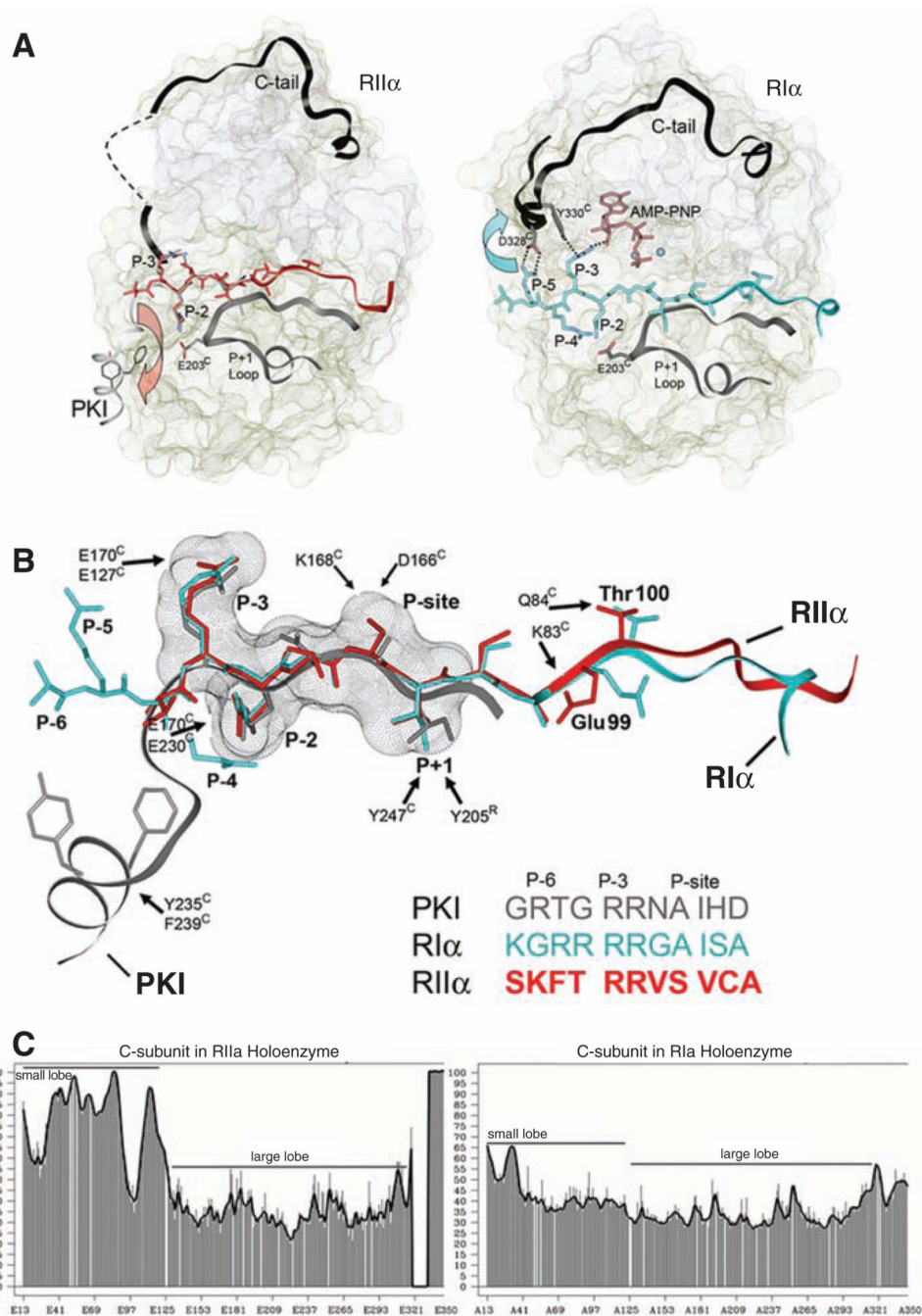


**Fig. 3.** Interactions of the inhibitor peptides with the active site. **(A)** The C subunits from RII $\alpha$  and RI $\alpha$  holoenzymes, as shown in a space-filling format, with the small lobes in gray and the large lobes in tan. Both C-terminal tails are shown as a black ribbon, and a dashed link points to the disordered region in RII $\alpha$ . The inhibitor peptides, in red for RII $\alpha$  and in cyan for RI $\alpha$ , are highlighted. We predict that the peptide of RII $\alpha$  will continue interacting with the large lobe, in a manner similar to PKI. However, this region in the RI $\alpha$  holoenzyme structure further anchors the C-terminal tail (11). **(B)** Superimposition of RII $\alpha$  peptide (in

red) with those of RI $\alpha$  (in cyan) and PKI (in gray). The regions from P-3 to P+1 are very similar, whereas their N-termini use different docking surfaces on C. Their sequence comparison is also shown (25). (C) *B*-factor plots of C in the RII $\alpha$  holoenzyme compared to the RI $\alpha$  holoenzyme. The *x* axis corresponds to the residue numbers; the *y* axis corresponds to the *B*-factor value scale.

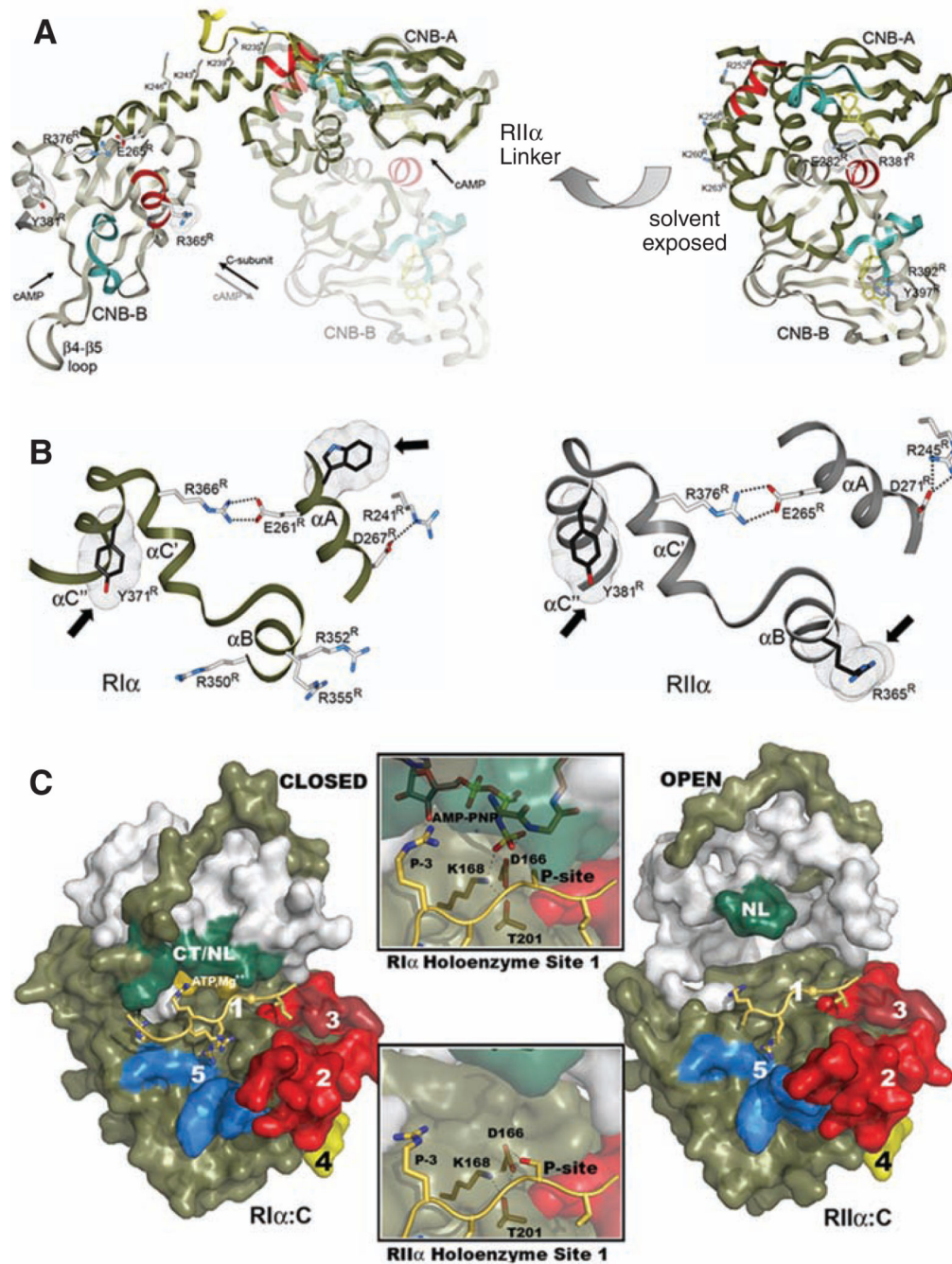


**Fig. 4.** Rearrangements of CNB domains. (A) Global change in domain B is due to the extension of the  $\alpha$ B- $\alpha$ C helix into a single long helix. There is a  $\sim 120^\circ$  flip from the cAMP-bound state (right) compared to its R-C complex state (left). The position of domain B in the cAMP-bound state is shown by a transparency on the left. The  $\alpha$ B helices from both CNBs, shown in red, are essential docking motifs. The PBCs are shown in dark green. Also labeled are the capping residues (Arg<sup>365</sup>R for site A and Tyr<sup>381</sup>R for site B), a salt bridge pair (Arg<sup>376</sup>R-Glu<sup>265</sup>R), and four basic residues that dock to the RII $\alpha$  linker. In the cAMP-bound state,

these basic residues are exposed to solvent. **(B)** The capping residues (shaded and indicated by arrows) for RI $\alpha$  and RII $\alpha$  in their holoenzyme conformation are far from their respective cAMP binding sites. A novel salt bridge (Arg<sup>366R</sup>-Glu<sup>261R</sup> for RI $\alpha$ , Arg<sup>376R</sup>-Glu<sup>265R</sup> for RII $\alpha$ ) is formed only upon holoenzyme formation. **(C)** The combinatorial diversity for the C subunit is demonstrated by shading the surface of the docking motifs that are used for binding different inhibitors (RI, RII, and PKI). Site 1, where the inhibitor peptide (yellow) docks, is essential for inhibition. Site 1 in each holoenzyme is expanded at the center of the panel. The other sites [N-lobe and C-tail in green,  $\alpha$ G helix (site 2) in red, activation loop (site 3) in dark red,  $\alpha$ H- $\alpha$ I loop (site 4) in yellow, and the  $\alpha$ F- $\alpha$ G loop (site 5) in blue] are used in a combinatorial fashion to achieve high-affinity binding.